

## LETTERS

# Targeted capture and massively parallel sequencing of 12 human exomes

Sarah B. Ng<sup>1</sup>, Emily H. Turner<sup>1</sup>, Peggy D. Robertson<sup>1</sup>, Steven D. Flygare<sup>1</sup>, Abigail W. Bigham<sup>2</sup>, Choli Lee<sup>1</sup>, Tristan Shaffer<sup>1</sup>, Michelle Wong<sup>1</sup>, Arindam Bhattacharjee<sup>4</sup>, Evan E. Eichler<sup>1,3</sup>, Michael Bamshad<sup>2</sup>, Deborah A. Nickerson<sup>1</sup> & Jay Shendure<sup>1</sup>

Genome-wide association studies suggest that common genetic variants explain only a modest fraction of heritable risk for common diseases, raising the question of whether rare variants account for a significant fraction of unexplained heritability<sup>1,2</sup>. Although DNA sequencing costs have fallen markedly<sup>3</sup>, they remain far from what is necessary for rare and novel variants to be routinely identified at a genome-wide scale in large cohorts. We have therefore sought to develop second-generation methods for targeted sequencing of all protein-coding regions ('exomes'), to reduce costs while enriching for discovery of highly penetrant variants. Here we report on the targeted capture and massively parallel sequencing of the exomes of 12 humans. These include eight HapMap individuals representing three populations<sup>4</sup>, and four unrelated individuals with a rare dominantly inherited disorder, Freeman–Sheldon syndrome (FSS)<sup>5</sup>. We demonstrate the sensitive and specific identification of rare and common variants in over 300 megabases of coding sequence. Using FSS as a proof-of-concept, we show that candidate genes for Mendelian disorders can be identified by exome sequencing of a small number of unrelated, affected individuals. This strategy may be extendable to diseases with more complex genetics through larger sample sizes and appropriate weighting of non-synonymous variants by predicted functional impact.

Protein-coding regions constitute ~1% of the human genome or ~30 megabases (Mb), split across ~180,000 exons. A brute-force approach to exome sequencing with conventional technology<sup>6</sup> is expensive relative to what may be possible with second-generation platforms<sup>3</sup>. However, the efficient isolation of this fragmentary genomic subset is technically challenging<sup>7</sup>. The enrichment of an exome by hybridization of shotgun libraries constructed from 140 µg of genomic DNA to seven microarrays was described previously<sup>8</sup>. To improve the practicality of hybridization capture, we developed a protocol to enrich for coding sequences at a genome-wide scale starting with 10 µg of DNA and using two microarrays. Our initial target was 27.9 Mb of coding sequence defined by CCDS (the NCBI Consensus Coding Sequence database)<sup>9</sup>. This curated set avoids the inclusion of spurious hypothetical genes that contaminate broader exome definitions<sup>10</sup>. The target is reduced to 26.6 Mb on exclusion of regions that are poorly mapped with our anticipated read length owing to paralogous sequences elsewhere in the genome (Supplementary Data 1).

We captured and sequenced the exomes of eight individuals previously characterized by the HapMap<sup>4</sup> and Human Genome Structural Variation<sup>11</sup> projects. We also analysed four unrelated individuals affected with Freeman–Sheldon syndrome (FSS; Online Mendelian Inheritance in Man (OMIM) #193700), also called distal arthrogyposis type 2A, a rare autosomal dominant disorder caused by

mutations in *MYH3* (ref. 5). Unpaired, 76 base-pair (bp) reads<sup>12</sup> from post-enrichment shotgun libraries were aligned to the reference genome<sup>13</sup>. On average, 6.4 gigabases (Gb) of mappable sequence was generated per individual (20-fold less than whole genome sequencing with the same platform<sup>12</sup>), and 49% of reads mapped to targets (Supplementary Table 1). After removing duplicate reads that represent potential polymerase chain reaction artefacts<sup>14</sup>, the average fold-coverage of each exome was 51× (Supplementary Fig. 1). On average per exome, 99.7% of targeted bases were covered at least once, and 96.3% (25.6 Mb) were covered sufficiently for variant calling ( $\geq 8\times$  coverage and Phred-like<sup>15</sup> consensus quality  $\geq 30$ ). This corresponded to 78% of genes having >95% of their coding bases called (Supplementary Fig. 2 and Supplementary Data 2). The average pairwise correlation coefficient between individuals for gene-by-gene coverage was 0.87, consistent with systematic bias in coverage between individual exomes.

False positives and false negatives are critical issues in genomic resequencing. We assessed the quality of our exome data in four ways. First, comparing sequence-based calls for the eight HapMap exomes to array-based genotyping, we observed a high concordance with both homozygous (99.94%;  $n = 219,077$ ) and heterozygous (99.57%;  $n = 43,070$ ) genotypes (Table 1). Second, we compared our coding single-nucleotide polymorphism (cSNP) catalogue to ~1 Mb of coding sequence determined in each of the eight HapMap individuals by molecular inversion probe (MIP) capture and direct resequencing<sup>16</sup>. At coordinates called in both data sets, 99.9% of all cSNPs ( $n = 4,620$ ) and 100% of novel cSNPs ( $n = 334$ ) identified here were concordant, consistent with a low false discovery rate. Third, we compared the NA18507 cSNPs identified here to those called by recent whole genome sequencing of this individual<sup>12</sup>, and found substantial overlap (Supplementary Fig. 3). The relative numbers of cSNPs called by only one approach, and the proportions of these represented in dbSNP, indicate that exome sequencing has equivalent sensitivity for cSNP detection compared to whole genome sequencing. Fourth, we compared our data to cSNPs in high-quality Sanger sequence of single haplotype regions from fosmid clones of the same HapMap individuals<sup>17</sup>. Most fosmid-defined cSNPs (38 of 40) were at coordinates with sufficient coverage in our data for variant calling. Of these, 38 of 38 were correctly identified as variant.

A comparison of our data to past reports on exonic<sup>18</sup> or exomic<sup>8</sup> array-based capture revealed roughly equivalent capture specificity, but greater completeness in terms of coverage and variant calling (Supplementary Table 2). These improvements probably arise from a combination of greater sequencing depth and differences in array designs and in experimental conditions for capture. Within the set of

<sup>1</sup>Department of Genome Sciences, <sup>2</sup>Department of Pediatrics, University of Washington, <sup>3</sup>Howard Hughes Medical Institute, Seattle, Washington 98195, USA. <sup>4</sup>Agilent Technologies, Santa Clara, California 95051, USA.

**Table 1 | Sequence coverage and array-based validation**

Individual	Covered $\geq 1\times$	Sequence called	Concordance with Illumina Human1M-Duo calls		
			Homozygous reference	Heterozygous	Homozygous non-reference
NA18507 (YRI)	26,477,161 (99.7%)	25,795,189 (97.1%)	23757/23762 (99.98%)	5553/5583 (99.46%)	3582/3592 (99.72%)
NA18517 (YRI)	26,476,761 (99.7%)	25,748,289 (97.0%)	23701/23705 (99.98%)	5575/5601 (99.54%)	3568/3579 (99.69%)
NA19129 (YRI)	26,491,035 (99.8%)	25,733,587 (96.9%)	23701/23708 (99.97%)	5482/5510 (99.49%)	3681/3690 (99.76%)
NA19240 (YRI)	26,486,481 (99.7%)	25,576,517 (96.3%)	23546/23551 (99.98%)	5600/5634 (99.40%)	3542/3549 (99.80%)
NA18555 (CHB)	26,475,665 (99.7%)	25,529,861 (96.1%)	23980/23984 (99.98%)	4877/4893 (99.67%)	3776/3786 (99.74%)
NA18956 (JPT)	26,454,942 (99.6%)	25,683,248 (96.7%)	24217/24221 (99.98%)	4890/4910 (99.59%)	3751/3760 (99.76%)
NA12156 (CEU)	26,476,155 (99.7%)	25,360,704 (95.5%)	23789/23794 (99.98%)	5493/5514 (99.62%)	3206/3213 (99.78%)
NA12878 (CEU)	26,439,953 (99.6%)	25,399,572 (95.6%)	23885/23891 (99.97%)	5413/5425 (99.78%)	3274/3292 (99.45%)
FSS10066 (Eur)	26,467,140 (99.7%)	25,546,738 (96.2%)	NA	NA	NA
FSS10208 (Eur)	26,461,768 (99.6%)	25,576,256 (96.3%)	NA	NA	NA
FSS22194 (Eur)	26,426,401 (99.5%)	25,454,551 (95.9%)	NA	NA	NA
FSS24895 (Eur)	26,478,775 (99.7%)	25,602,677 (96.4%)	NA	NA	NA

The number of coding bases covered at least  $1\times$  and with sufficient coverage to variant call ( $\geq 8\times$  and consensus quality  $\geq 30$ ) are listed for each exome, with the fraction of the aggregate target (26.6 Mb) that this represents in parentheses. For the eight HapMap individuals, concordance with array genotyping (Illumina Human1M-Duo) is listed for positions that are homozygous for the reference allele, heterozygous or homozygous for the non-reference allele (according to the array genotype). CEU, CEPH HapMap; CHB, Chinese HapMap; Eur, European-American ancestry (non-HapMap); JPT, Japanese HapMap; YRI, Yoruba HapMap. NA, Not applicable.

called positions, the high concordance with heterozygous array-based genotypes ( $>99\%$ ) provides an estimate of our sensitivity for rare variant detection, as rare variants are overwhelmingly expected to be heterozygous. However, sensitivity was limited in that  $\sim 4\%$  of known heterozygous genotypes were at coordinates where there was insufficient coverage to make a confident call.

There were 56,240 cSNPs called in one or more individuals, of which 13,347 were novel. On average, 17,272 cSNPs were called per individual, of which 92% were already annotated in a public database (dbSNP v129) (Table 2a). The proportion of previously annotated cSNPs was consistent by population, and higher for European (94%;  $n = 6$ ) and Asian (93%;  $n = 2$ ) than Yoruba (88%;  $n = 4$ ) ancestry. These confirmation rates are  $\sim 10\%$  higher than recent whole genome analyses<sup>12,19–22</sup>. The most likely explanation is that coding sequences have historically been more heavily ascertained than noncoding sequences, although other factors such as dbSNP version, prior ascertainment of HapMap individuals and different false discovery rates may contribute as well. For the subset of cSNPs at coordinates with sufficient coverage for variant calling in all 12 individuals

( $n = 47,079$ ), 32% of annotated variants and 86% of novel variants were singleton observations across 24 chromosomes (Fig. 1a).

We also estimated the total number of cSNPs in each individual relative to the reference genome (Table 2b). As the precise and comprehensive definition of the human exome remains incomplete, we extrapolated our data to an estimated exome size of exactly 30 Mb. The results were remarkably consistent by population. As expected, a higher number of non-synonymous cSNPs were estimated for the Yoruba individuals (average 10,254;  $n = 4$ ) than non-Africans (average 8,489;  $n = 8$ ). More heterozygous cSNPs were estimated for the four Yoruba (average 14,995) than the six European Americans (average 11,586) and the two Asians (average 10,631). The ratio of synonymous to non-synonymous cSNPs was 1.2 within any single individual, and 1.1 when calculated for a non-redundant list of variants identified across all individuals. The difference results from the slightly shifted allele frequency distribution of non-synonymous variants (Fig. 1b). Consistent with expectation<sup>23</sup>, the trend is more pronounced for non-synonymous variants predicted to be damaging (by PolyPhen<sup>24</sup>) (Fig. 1c).

**Table 2 | Coding variation across 12 human exomes****a** Summary statistics for observed cSNPs

Individual	cSNP calls	Number in dbSNP	Percentage in dbSNP	Number heterozygous	Number homozygous
NA18507 (YRI)	19,720	17,577	89.1	12,896	6,824
NA18517 (YRI)	19,737	17,326	87.8	13,039	6,698
NA19129 (YRI)	19,761	17,298	87.5	12,845	6,916
NA19240 (YRI)	19,517	17,168	88.0	12,866	6,651
NA18555 (CHB)	16,047	14,894	92.8	9,181	6,866
NA18956 (JPT)	16,011	14,848	92.7	9,132	6,879
NA12156 (CEU)	16,119	15,250	94.6	10,179	5,940
NA12878 (CEU)	15,970	15,051	94.2	9,928	6,042
FSS10066 (Eur)	16,229	15,144	93.3	10,240	5,989
FSS10208 (Eur)	16,073	15,018	93.4	9,966	6,107
FSS22194 (Eur)	16,094	15,128	94.0	10,005	6,089
FSS24895 (Eur)	15,986	15,027	94.0	9,920	6,066

**b** Genome-wide cSNP estimates assuming a 30 Mb exome

Individual	Estimated total cSNPs	Estimated total heterozygous	Estimated total homozygous	Estimated total synonymous	Estimated total non-synonymous
NA18507 (YRI)	22,727	14,876	7,851	12,466	10,261
NA18517 (YRI)	22,841	15,135	7,706	12,550	10,291
NA19129 (YRI)	22,907	14,906	8,001	12,693	10,214
NA19240 (YRI)	22,814	15,063	7,751	12,565	10,249
NA18555 (CHB)	18,722	10,677	8,045	10,275	8,447
NA18956 (JPT)	18,523	10,585	7,938	10,072	8,451
NA12156 (CEU)	18,825	11,818	7,007	10,220	8,605
NA12878 (CEU)	18,544	11,455	7,089	10,110	8,434
FSS10066 (Eur)	18,836	11,795	7,041	10,240	8,596
FSS10208 (Eur)	18,591	11,444	7,147	10,075	8,516
FSS22194 (Eur)	18,667	11,539	7,128	10,144	8,523
FSS24895 (Eur)	18,508	11,466	7,042	10,169	8,339

For part **a**, cSNPs called in each individual, relative to the reference genome, are broken down by the fraction in dbSNP and by genotype. Part **b** shows extrapolation of observed numbers of cSNPs in each individual to an exactly 30 Mb exome. CEU, CEPH HapMap; CHB, Chinese HapMap; Eur, European-American ancestry (non-HapMap); JPT, Japanese HapMap; YRI, Yoruba HapMap.

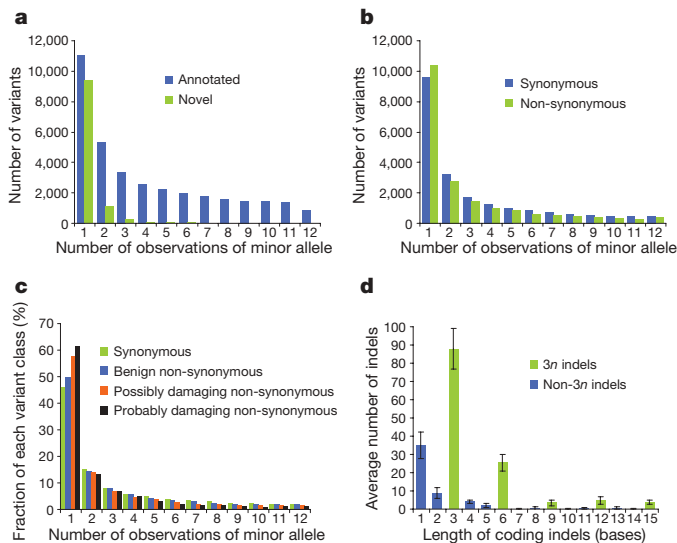


**Figure 1 | Minor allele frequency and coding indel length distributions.** **a**, The distribution of minor allele frequencies is shown for previously annotated versus novel cSNPs. **b**, The distribution of minor allele frequencies is shown for synonymous versus non-synonymous cSNPs. **c**, The distribution of minor allele frequencies (by proportion, rather than count) is shown for synonymous cSNPs ( $n = 21,201$ ) versus non-synonymous cSNPs predicted to be benign ( $n = 13,295$ ), possibly damaging ( $n = 3,368$ ), or probably damaging ( $n = 2,227$ ) by PolyPhen<sup>24</sup>. **d**, The distribution of lengths of coding indel variants is shown (average numbers per exome). Error bars indicate s.d.

Nonsense mutations and splice-site disruptions are often assumed to be deleterious, but have a broad range of potential fitness effects<sup>25–27</sup>. Our non-redundant cSNP catalogue included 225 nonsense mutations (112 novel) and 102 splice-site disruptions (49 novel). Excluding 86 nonsense alleles that are common in this data set (two or more observations) or in a recent study<sup>25</sup> (>5% allele frequency), our genome-wide estimate (projected to 30 Mb) for the average number of relatively rare mutations introducing premature nonsense codons in an individual genome was 10 for non-Africans ( $n = 8$ ) and 20 for Yoruba ( $n = 4$ ). However, these are probably overestimates, given that our catalogue of common nonsense mutations remains incomplete.

Short insertions and deletions (indels) in coding sequence are likely to be functionally important when they cause frameshifts, but are difficult to detect with short reads. We developed and applied an approach for identifying indels from our unpaired 76 bp reads. In total, 664 coding indels were called in one or more individuals. On average, 166 coding indels were called per individual, of which 63% were previously annotated in dbSNP (Supplementary Table 3). To assess our sensitivity, we compared our data for NA18507 to data published previously<sup>12</sup>. The majority (73%) of their coding indels were also observed in our data (136 of 187). To assess specificity, we attempted PCR and Sanger sequencing of 28 novel coding indels chosen at random. Of 21 successful assays, 20 coding indels were verified and 1 was a false positive. We anticipate that future use of paired-end reads will improve detection of coding indels.

The shape of the distribution of coding indel lengths was consistent with other studies<sup>10,20</sup> as well as across the 12 exomes (Fig. 1d), demonstrating a preference for multiples of 3 ('3n'). Of the 664 coding indels observed here, 65% were 3n in length. The allele frequency distribution for novel indels relative to annotated indels was markedly shifted towards rarer variants (Supplementary Fig. 4). However, the length histograms for novel versus annotated coding indels were similar (Supplementary Fig. 5), reinforcing the notion that our set of novel coding indels is not excessively contaminated with false positives (as these would not be expected to have the observed 3n bias). Excluding indels that were common in this data

set (two or more observations), the average number of relatively rare frameshifting indels identified per individual was 8 for non-Africans ( $n = 8$ ) and 17 for Yoruba ( $n = 4$ ).

The number of synonymous, missense, nonsense, splice site, frameshifting indel and non-frameshifting indel variants observed in each individual (as well as the size of the subsets that are novel and singleton observations) is presented in Supplementary Table 4. Also shown are the average numbers of variants of each class for non-Africans and Yoruba.

Phenotypes inherited in an apparently Mendelian pattern often lack sufficiently sized pedigrees to pinpoint the causal locus. We evaluated whether exome sequencing could be applied to identify directly the causative gene underlying a monogenic human disease (FSS), that is, with neither linkage data nor candidate gene analysis. Even in this simple scenario for 'whole exome/genome genetics', the key challenge that arises immediately is that the large number of apparently private mutations present by chance in any single human genome makes it difficult to identify which variant is causal, even when only considering non-synonymous variants. This hurdle was overcome recently in the context of hereditary pancreatic cancer by restricting focus only to nonsense mutations and also resequencing tumour DNA from the same individual, but this approach greatly limits sensitivity and is only relevant to a subset of mechanisms within one disease class<sup>28</sup>.

To quantify this background of non-causal variants in our exome data, we first investigated how many genes had one or more non-synonymous cSNPs, splice site disruptions or coding indels in one or several FSS exomes (Fig. 2, row 1). Simply requiring that a gene contain variants in multiple affected individuals was clearly insufficient, as over 2,000 candidate genes remained even after intersecting four FSS exomes. We then applied filters to remove presumably common variants, as these are unlikely to be causative. Removing dbSNP-catalogued variants from consideration reduced the number of candidates considerably (Fig. 2, row 2). Remarkably, the eight HapMap exomes provided a filter nearly equivalent to dbSNP (Fig. 2, row 3). Combining the two catalogues had a synergistic effect (Fig. 2, row 4), such that the candidate list could be narrowed to a single gene (*MYH3*, identified previously by a candidate gene approach as causative for FSS<sup>5</sup>). Specifically, *MYH3* is the only gene where: (1) at least one (but not necessarily the same) non-synonymous cSNP, splice-site disruption or coding indel is observed in all four individuals with FSS; (2) the mutations are not in dbSNP, nor in the eight HapMap exomes. Taking the predicted deleteriousness of individual mutations into account served as an effective filter as well (Fig. 2, row 5), but was not required to identify *MYH3*. Ranges

	FSS24895	FSS24895 FSS10208	FSS24895 FSS10208 FSS10066	FSS24895 FSS10208 FSS10066 FSS22194	Any 3 of 4 FSS24895 FSS10208 FSS10066 FSS22194
Non-synonymous cSNP, splice site variant or coding indel (NS/SS/I)	4,510	3,284	2,765	2,479	3,768
NS/SS/I not in dbSNP	513	128	71	53	119
NS/SS/I not in eight HapMap exomes	799	168	53	21	160
NS/SS/I neither in dbSNP nor eight HapMap exomes	360	38	8	1 ( <i>MYH3</i> )	22
...And predicted to be damaging	160	10	2	1 ( <i>MYH3</i> )	3

**Figure 2 | Direct identification of the causal gene for a monogenic disorder by exome sequencing.** Boxes list the number of genes with one or more non-synonymous cSNP, splice-site SNP, or coding indel (NS/SS/I) meeting specified filters. Columns show the effect of requiring that one or more NS/SS/I variants be observed in each of one to four affected individuals. Rows show the effect of excluding from consideration variants found in dbSNP, the eight HapMap exomes, or both. Column five models limited genetic heterogeneity or data incompleteness by relaxing criteria such that variants need only be observed in any three of four exomes for a gene to qualify.

of candidate list sizes when other permutations of individuals are used are shown in Supplementary Fig. 6.

*MYH3* was well covered in our data. To assess our sensitivity more globally, we calculated the probability that a mutation would have been identified in all four FSS-affected individuals for each gene, based on our overall coverage of that gene in each individual (Supplementary Data 2). The average probability across all genes was 86%. This is probably still an overestimate of sensitivity, as functional noncoding or structural mutations would be missed. It also remains challenging to detect mutations in segmentally duplicated regions of the genome with short read sequencing.

Nevertheless, our analysis suggests that direct sequencing of exomes of small numbers of unrelated individuals (but more than one) with a shared monogenic disorder can serve as a genome-wide scan for the causative gene. The availability of the eight HapMap exomes was clearly helpful, suggesting that the power of this approach will improve as the 1000 Genomes Project<sup>29</sup> generates a catalogue of common variation that is more complete and evenly ascertained than dbSNP. Also, FSS is inherited in an autosomal dominant pattern so the presence of only one mutant allele is sufficient to cause disease. Applying this strategy to a recessive disease would probably be easier, because there are far fewer genes in each exome that are homozygous or compound heterozygous for rare non-synonymous variants. We also note that modelling of even a modest degree of genetic heterogeneity or data incompleteness is observed to have a significant impact on performance (Fig. 2, column offset to the right). Moving along the spectrum from rare monogenic disorders to complex common diseases, it is likely that the increasing extent of genetic heterogeneity will need to be matched by increasingly large sample sizes<sup>30</sup>, and/or more sophisticated weighting of predicted mutational impact.

A clear limitation of exome sequencing is that it does not identify the structural and noncoding variants found by whole genome sequencing. At the same time, it allows a given amount of sequencing to be extended across at least 20 times as many samples compared to whole genome sequencing. In studies focused on identifying rare variants or somatic mutations with medical relevance, sample size and the interpretability of functional impact may be critical to achieving meaningful success. It is in the context of such studies that exome sequencing may be most valuable.

We demonstrate that targeted capture and massively parallel sequencing represents a cost-effective, reproducible and robust strategy for the sensitive and specific identification of variants causing protein-coding changes in individual human genomes. The 307 Mb determined here across 12 individuals is the largest data set reported so far of human coding sequence ascertained by second-generation sequencing methods. Finally, our successful demonstration that the causative gene for a Mendelian disorder can be identified directly by exome sequencing of several unrelated individuals provides increasing context to the possibility that exome or genome sequencing may represent a new approach for identifying gene–disease relationships.

## METHODS SUMMARY

**DNA samples, targeted capture and massively parallel sequencing.** DNA samples were obtained from Coriell Repositories (HapMap) or by M.B. (FSS). Each shotgun library was hybridized to two Agilent 244K microarrays for target enrichment, followed by washing, elution and additional amplification. The first array targeted CCDS (2007), while the second was designed against targets poorly captured by the first array plus updates to CCDS in 2008. All sequencing was performed on the Illumina GA2 platform. Oligonucleotides used are listed in Supplementary Table 5.

**Read mapping and variant analysis.** Reads were mapped to the reference human genome (hg18, downloaded from <http://genome.ucsc.edu>), initially with ELAND (Illumina) for quality recalibration, and then again with Maq<sup>13</sup>. Sequence calls were also performed by Maq, and filtered to coordinates with  $\geq 8\times$  coverage and a Phred-like<sup>15</sup> consensus quality  $\geq 30$ . Sequence calls for HapMap individuals were compared against Illumina Human1M-Duo genotypes. NA18507 SNPs from whole genome data<sup>12</sup> were obtained from

Illumina. Annotations of cSNPs were based on NCBI and UCSC databases, supplemented with PolyPhen Grid Gateway<sup>24</sup> predictions for non-synonymous SNPs.

**Identification of coding indels.** Identification of coding indels involved: (1) gapped alignment of unmapped reads to the genome to generate a set of candidate indels using *cross\_match*; (2) ungapped alignment of all reads to the reference and alternative alleles for all candidate indels using *Maq*; and (3) filtering by coverage and allelic ratio.

**Data access.** Sequencing reads for HapMap individuals are available from the NCBI Short Read Archive, accession SRP000910. Variants identified in HapMap individuals have been submitted to NCBI dbSNP under the handle 'SEATTLESEQ'. Variants identified in FSS individuals are available to approved investigators through NCBI dbGaP, accession number phs000204. Individual genotypes for variants identified in HapMap individuals, as well as the collapsed CCDS 2008 definition (before masking of coordinates listed in Supplementary Data 1), are available at [http://krishna.gs.washington.edu/12\\_exomes](http://krishna.gs.washington.edu/12_exomes).

**Full Methods** and any associated references are available in the online version of the paper at [www.nature.com/nature](http://www.nature.com/nature).

Received 5 June; accepted 29 June 2009.

Published online 16 August 2009.

- Cohen, J. C. *et al.* Multiple rare alleles contribute to low plasma levels of HDL cholesterol. *Science* **305**, 869–872 (2004).
- Frazer, K. A., Murray, S. S., Schork, N. J. & Topol, E. J. Human genetic variation and its contribution to complex traits. *Nature Rev. Genet.* **10**, 241–251 (2009).
- Shendure, J. & Ji, H. Next-generation DNA sequencing. *Nature Biotechnol.* **26**, 1135–1145 (2008).
- The International HapMap Consortium. A haplotype map of the human genome. *Nature* **437**, 1299–1320 (2005).
- Toydemir, R. M. *et al.* Mutations in embryonic myosin heavy chain (*MYH3*) cause Freeman-Sheldon syndrome and Sheldon-Hall syndrome. *Nature Genet.* **38**, 561–565 (2006).
- Sjblom, T. *et al.* The consensus coding sequences of human breast and colorectal cancers. *Science* **314**, 268–274 (2006).
- Olson, M. Enrichment of super-sized resequencing targets from the human genome. *Nature Methods* **4**, 891–892 (2007).
- Hodges, E. *et al.* Genome-wide *in situ* exon capture for selective resequencing. *Nature Genet.* **39**, 1522–1527 (2007).
- National Center for Biotechnology Information. Consensus CDS protein set <<http://www.ncbi.nlm.nih.gov/projects/CCDS>> (2009).
- Ng, P. C. *et al.* Genetic variation in an individual human exome. *PLoS Genet.* **4**, e1000160 (2008).
- Kidd, J. M. *et al.* Mapping and sequencing of structural variation from eight human genomes. *Nature* **453**, 56–64 (2008).
- Bentley, D. R. *et al.* Accurate whole human genome sequencing using reversible terminator chemistry. *Nature* **456**, 53–59 (2008).
- Li, H., Ruan, J. & Durbin, R. Mapping short DNA sequencing reads and calling variants using mapping quality scores. *Genome Res.* **18**, 1851–1858 (2008).
- Campbell, P. J. *et al.* Identification of somatically acquired rearrangements in cancer using genome-wide massively parallel paired-end sequencing. *Nature Genet.* **40**, 722–729 (2008).
- Ewing, B. & Green, P. Base-calling of automated sequencer traces using *Phred*. II. Error probabilities. *Genome Res.* **8**, 186–194 (1998).
- Turner, E. H., Lee, C., Ng, S. B. & Shendure, J. Massively parallel exon capture and library-free resequencing across 16 individuals. *Nature Methods* **6**, 315–316 (2009).
- Kidd, J. M. *et al.* Haplotype sorting using human fosmid clone end-sequence pairs. *Genome Res.* **18**, 2016–2023 (2008).
- Albert, T. J. *et al.* Direct selection of human genomic loci by microarray hybridization. *Nature Methods* **4**, 903–905 (2007).
- Wheeler, D. A. *et al.* The complete genome of an individual by massively parallel DNA sequencing. *Nature* **452**, 872–876 (2008).
- Wang, J. *et al.* The diploid genome sequence of an Asian individual. *Nature* **456**, 60–65 (2008).
- Levy, S. *et al.* The diploid genome sequence of an individual human. *PLoS Biol.* **5**, e254 (2007).
- Ley, T. J. *et al.* DNA sequencing of a cytogenetically normal acute myeloid leukaemia genome. *Nature* **456**, 66–72 (2008).
- Boyko, A. R. *et al.* Assessing the evolutionary impact of amino acid mutations in the human genome. *PLoS Genet.* **4**, e1000083 (2008).
- Sunyaev, S. *et al.* Prediction of deleterious human alleles. *Hum. Mol. Genet.* **10**, 591–597 (2001).
- Yngvadottir, B. *et al.* A genome-wide survey of the prevalence and evolutionary forces acting on human nonsense SNPs. *Am. J. Hum. Genet.* **84**, 224–234 (2009).
- Olson, M. V. When less is more: gene loss as an engine of evolutionary change. *Am. J. Hum. Genet.* **64**, 18–23 (1999).
- Cohen, J. *et al.* Low LDL cholesterol in individuals of African descent resulting from frequent nonsense mutations in *PCSK9*. *Nature Genet.* **37**, 161–165 (2005).

28. Jones, S. *et al.* Exomic sequencing identifies *PALB2* as a pancreatic cancer susceptibility gene. *Science* **324**, 217 (2009).
29. Siva, N. 1000 Genomes project. *Nature Biotechnol.* **26**, 256 (2008).
30. Kryukov, G. V., Shpunt, A., Stamatoyannopoulos, J. A. & Sunyaev, S. R. Power of deep, all-exon resequencing for discovery of human trait genes. *Proc. Natl Acad. Sci. USA* **106**, 3871–3876 (2009).

**Supplementary Information** is linked to the online version of the paper at [www.nature.com/nature](http://www.nature.com/nature).

**Acknowledgements** For discussions or assistance with genotyping data, we thank P. Green, J. Akey, R. Patwardhan, G. Cooper, J. Kidd, D. Gordon, J. Smith, I. Stanaway and M. Rieder. For assistance with project management, computation, data management and submission, we thank E. Torskey, S. Thompson, T. Amburg, B. McNally, S. Hearsey, M. Shumway and L. Hillier. For Human1M-Duo genotype data on HapMap samples, we thank Illumina. Our work was supported in part by grants from the National Institutes of Health/National Heart Lung and Blood Institute, the National Institutes of Health/National Human Genome Research

Institute, National Institutes of Health/National Institute of Child Health and Human Development, and the Washington Research Foundation. S.B.N. is supported by the Agency for Science, Technology and Research, Singapore. E.H.T. and A.W.B. are supported by a training fellowship from the National Institutes of Health/National Human Genome Research Institute. E.E.E. is an investigator of the Howard Hughes Medical Institute.

**Author Contributions** The project was conceived and experiments planned by S.B.N., E.H.T., A.B., E.E.E., M.B., D.A.N. and J.S. Experiments were performed by S.B.N., E.H.T., C.L. and M.W. Algorithm development and data analysis were performed by S.B.N., P.D.R., S.D.F., A.W.B., T.S., M.B., D.A.N. and J.S. The manuscript was written by S.B.N. and J.S. All aspects of the study were supervised by J.S.

**Author Information** Reprints and permissions information is available at [www.nature.com/reprints](http://www.nature.com/reprints). The authors declare competing financial interests: details accompany the full-text HTML version of the paper at [www.nature.com/nature](http://www.nature.com/nature). Correspondence and requests for materials should be addressed to J.S. ([shendure@u.washington.edu](mailto:shendure@u.washington.edu)) or S.B.N. ([sarahng@u.washington.edu](mailto:sarahng@u.washington.edu)).

## METHODS

**Genomic DNA samples.** Targeted capture was performed on genomic DNA from eight HapMap individuals (four Yoruba (NA18507, NA18517, NA19129 and NA19240), two East Asians (NA18555 and NA18956) and two European-Americans (NA12156 and NA12878)) and four European-American individuals affected by Freeman–Sheldon syndrome (FSS10066, FSS10208, FSS22194 and FSS24895). Genomic DNA for HapMap individuals was obtained from Coriell Cell Repositories. Genomic DNA for FSS individuals was obtained by M.B.

**Oligonucleotides and adaptors.** All oligonucleotides were synthesized by Integrated DNA Technologies and resuspended in nuclease-free water to a stock concentration of 100  $\mu$ M. Sequences are shown in Supplementary Table 5. Double-stranded library adaptors SLXA\_1 and SLXA\_2 were prepared to a final concentration of 50  $\mu$ M by incubating equimolar amounts of SLXA\_1\_HI and SLXA\_1\_LO together and SLXA\_2\_HI and SLXA\_2\_LO together at 95 °C for 3 min and then leaving the adaptors to cool to room temperature in the heat block.

**Shotgun library construction.** Shotgun libraries were generated from 10  $\mu$ g of genomic DNA (gDNA) using protocols modified from the standard Illumina protocol<sup>12</sup>. Each library provided sufficient material for hybridization to two microarrays. For each sample, gDNA in 300  $\mu$ l 1 $\times$  Tris-EDTA was first sonicated for 30 min using a Bioruptor (Diagenode) set at high, then end-repaired for 45 min in a 100  $\mu$ l reaction volume using 1 $\times$  End-It Buffer, 10  $\mu$ l dNTP mix and 10  $\mu$ l ATP as supplied in the End-It DNA End-Repair Kit (Epicentre). The fragments were then A-tailed for 20 min at 70 °C in a 100  $\mu$ l reaction volume with 1 $\times$  PCR buffer (Applied Biosystems), 1.5 mM MgCl<sub>2</sub>, 1 mM dATP and 5 U AmpliTaq DNA polymerase (Applied Biosystems). Next, library adaptors SLXA\_1 and SLXA\_2 were ligated to the A-tailed sample in a 90  $\mu$ l reaction volume with 1 $\times$  Quick Ligation Buffer (New England Biolabs) with 5  $\mu$ l Quick T4 DNA Ligase (New England Biolabs) and each adaptor in 10 $\times$  molar excess of sample. Samples were purified on QIAquick columns (Qiagen) after each of these four steps and DNA concentration determined on a Nanodrop-1000 (Thermo Scientific) when necessary.

Each sample was subsequently size-selected for fragments of size 150–250 bp using gel electrophoresis on a 6% TBE-polyacrylamide gel (Invitrogen). A gel slice containing the fragments of interest was then excised and transferred to a siliconized 0.5 ml microcentrifuge tube (Ambion) with a 20 G needle-punched hole in the bottom. This tube was placed in a 1.5 ml siliconized microcentrifuge tube (Ambion), and centrifuged in a tabletop microcentrifuge at 16,110g for 5 min to create a gel slurry that was then resuspended in 200  $\mu$ l 1 $\times$  Tris-EDTA and incubated at 65 °C for 2 h, with periodic vortexing. This allowed for passive elution of DNA, and the aqueous phase was then separated from gel fragments by centrifugation through 0.2  $\mu$ m NanoSep columns (Pall Life Sciences) and the DNA recovered using a standard ethanol precipitation.

Recovered DNA was resuspended in elution buffer (EB; 10 mM Tris-Cl, pH 8.5, Qiagen) and the entire volume used in a 1 ml bulk PCR reaction volume with 1 $\times$  iProof High-Fidelity Master Mix (Bio-Rad) and 0.5  $\mu$ M each of primers SLXA\_FOR\_AMP and SLXA\_REV\_AMP with the conditions: 98 °C for 30 s, 20 cycles at 98 °C for 30 s, 65 °C for 10 s and 72 °C for 30 s, and finally 72 °C for 5 min. PCR products were purified across four QIAquick columns (Qiagen) and all the eluants pooled.

**Design of exome capture arrays.** We targeted all well-annotated protein-coding regions as defined by the CCDS (version 20080902). Coordinates were extracted from entries with ‘public’ status, and regions with overlapping coordinates were merged. This resulted in a target with 164,007 discontinuous regions summing to 27,931,548 bp. By comparison, coding sequence defined by all of RefSeq (NCBI 36.3) comprises 31.9 Mb (14% larger). Hybridization probes against the target were designed primarily such that they were evenly spaced across each region. Probes were also constrained (1) to be relatively unique, such that the average occurrence of each 15-mer in the probe sequence is less than 100<sup>8</sup>, (2) to be between 20 and 60 bases in length, with preference for longer probes, and (3) to have a calculated melting temperature ( $T_m$ )  $\leq$  69 °C, with preference for higher  $T_m$  values.  $T_m$  was calculated by  $64.9 + 41 \times (\text{number of G + Cs} - 16.4)/\text{length of probe}$ .

Two arrays (Agilent, 244K format) were designed and used per individual. The first array was common to all individuals, and contained 241,071 probes designed mainly against the subset of the target that was also found in a previous version of the CCDS (CCDS20070227). For most exomes, the second array was custom-designed specifically against target regions that had not been adequately represented after capture on the first array and subsequent sequencing. For two individuals (FSS10066, FSS10208), the matching was to a different individual’s first-array data. However, this did not seem to have a significant effect on performance, probably because features capturing poorly on the first array largely did so consistently. Additionally, all of the second arrays also targeted sequences

found in CCDS20080902 that were not in CCDS20070227 and hence not targeted by the first array. A subset of arrays used lacked control grids.

**Targeted capture by hybridization to DNA microarrays.** Hybridizations to Agilent 244K arrays were performed following manufacturer’s instructions with modifications. For each enrichment, a 520  $\mu$ l hybridization solution containing 20  $\mu$ g of the bulk-amplified genomic DNA library, 1 $\times$  aCGH hybridization buffer (Agilent), 1 $\times$  blocking agent (Agilent), 50  $\mu$ g human CotI DNA (Invitrogen) and 0.92 nmol each of the blocking oligonucleotides SLXA\_FOR\_AMP, SLXA\_REV\_AMP, SLXA\_FOR\_AMP\_rev and SLXA\_REV\_AMP\_rev was incubated at 95 °C for 3 min and then at 37 °C for at least 30 min. The hybridization solution was then loaded and the hybridization chamber assembled following the manufacturer’s instructions. Incubation was done at 65 °C for at least 66 h with rotation at 20 r.p.m. in a hybridization oven (Agilent).

After hybridization, the slide-gasket sandwich was removed from the chamber and placed in a 50 ml conical tube filled with aCGH Wash Buffer 1 (Agilent). The slide was separated from the gasket while in the buffer and then washed, first with fresh aCGH Wash Buffer 1 at room temperature for 10 min on an orbital shaker (VWR) set on low speed, and then in pre-warmed aCGH Wash Buffer 2 (Agilent) at 37 °C for 5 min. Both washes were also done in 50 ml conical tubes.

A Secure-Seal (SA2260, Grace Bio Labs) was then affixed firmly over the active area of the washed slide and heated briefly according to the manufacturer’s instructions. One port was sealed with a seal tab and the seal chamber completely filled with approximately 1 ml of hot EB (95 °C). The other port was sealed and the slide incubated at 95 °C on a heat block. After 5 min, one port was unsealed and the solution recovered. DNA was purified from the solution using a standard ethanol precipitation.

Precipitated DNA was resuspended in EB and the entire volume used in a 50  $\mu$ l PCR volume comprising of 1 $\times$  iTaq SYBR Green Supermix with ROX (Bio-Rad) and 0.2  $\mu$ M each of primers SLXA\_FOR\_AMP and SLXA\_REV\_AMP. Thermal cycling was done in a MiniOpticon Real-time PCR system (Bio-Rad) with the following programme: 95 °C for 5 min, then 30 cycles of 95 °C for 30 s, 55 °C for 2 min and 72 °C for 2 min. Each sample was monitored and extracted from the PCR machine when fluorescence began to plateau. Samples were then purified on a QIAquick column (Qiagen) and sequenced.

**Sequencing.** All sequencing of post-enrichment shotgun libraries was carried out on an Illumina Genome Analyzer II as single-end 76 bp reads, following the manufacturer’s protocols and using the standard sequencing primer. Image analysis and base calling was performed by the Genome Analyser Pipeline version 1.0 or 1.3 with default parameters, but with no pre-filtering of reads by quality. Quality values were recalibrated by alignment to the reference human genome with the Eland module.

**Read mapping.** The reference human genome used in these analyses was UCSC assembly hg18 (NCBI build 36.1), including unordered sequence (chrN\_random.fa) but not including alternate haplotypes. For each lane, reads with calibrated qualities were extracted from the Eland export output. Base qualities were rescaled and reads mapped to the human reference genome using Maq (version 0.7.1)<sup>13</sup>. Unmapped reads were dumped using the  $-u$  option and subsequently used for indel mapping. Mapped reads that overlapped target regions (‘target reads’) were used for all other analyses.

**Target masking.** All possible 76-bp reads that overlapped the aggregate target were simulated, mapped using Maq and consensus called using Maq assemble with parameters  $-q 1 -r 0.2 -t 0.9$ . Target coordinates that had read depth  $< 76$  (that is, half of the expected depth), reflecting a poor ability to have reads confidently mapped to them (Supplementary Data 1), were removed from consideration for downstream analyses, leaving a 26,553,795 bp target.

**Variant calling.** All reads with a map score  $> 0$  from each individual were merged and filtered for duplicates such that only the read with the highest aggregate base quality at any given start position and orientation was retained. Sequence calls were obtained using Maq assemble with parameters  $-r 0.2 -t 0.9$ , and only coordinates with at least 8 $\times$  coverage and an estimated Phred-like consensus quality value of at least 30 were used for downstream variant analyses.

**Comparison of sequence calls to array genotypes, dbSNP and whole genome sequencing.** For the eight HapMap individuals, sequence calls were compared to array-based genotyping data (Illumina Human1M-Duo) provided by Illumina. We excluded from consideration genotyping assays where all eight individuals were called by the arrays as homozygous non-reference as well as the MHC locus at chromosome 6:32500001–33300000, as both sets are likely to be error-enriched in the genotyping data. We downloaded dbSNP(v129) from [ftp://ftp.ncbi.nih.gov/snp/organisms/human\\_9606/chr\\_rpts](ftp://ftp.ncbi.nih.gov/snp/organisms/human_9606/chr_rpts) on 13 May 2008. Approximately 14.2 million non-redundant coordinates were defined by this file set. For comparison of NA18507 cSNPs to whole genome data, variant lists were obtained from Illumina<sup>12</sup>.

**Identification of coding indels.** Reads for which Maq was unsuccessful in identifying an ungapped alignment were converted to fasta format and mapped to the

human reference genome with `cross_match` (v1.080812, <http://www.phrap.org>), using parameters `-gap_ext -1 -bandwidth 10 -minmatch 20 -maxmatch 24`. Output options `-tags -discrep_lists -alignments -score_hist` were also set. Alignments with an indel were then filtered for those that: (1) had a score at least 40 more than the next best alignment; (2) mapped at least 75 bases of the read; (3) had no substitutions in addition to the indel; and (4) overlapped a target region. Reads from filtered alignments that mapped to the negative strand were then reverse-complemented and, together with the rest of the filtered reads, re-mapped with `cross_match` using the same parameters. This was to reduce ambiguity in called indel positions due to different read orientations. After the second mapping, alignments were re-filtered using the same criteria (1) to (4). For each sample, a putative indel event was called if at least two filtered reads covered the same event. A fasta file containing the sequences of all called events  $\pm 75$  bp, as well as the reference sequence at the same positions, was then generated for each individual. All the reads from each individual were then mapped to its 'indel reference' with `Maq` using default parameters. Reads that mapped multiple times (map score 0) or had redundant start sites were removed, after which the number of reads mapping to either the reference or the non-reference allele was counted for each individual and indel. An indel was called if there were at least eight non-reference allele reads making up at least 30% of all reads at that genomic position. Indels were called as heterozygous if non-reference alleles were 30–70% of reads at that position, and homozygous non-reference if  $>70\%$ .

**Variant annotation.** For cSNP annotation, we constructed a local server that integrates data from NCBI (including dbSNP and Consensus CDS files) and from UCSC Genome Bioinformatics. We also generated PolyPhen predictions<sup>24</sup> for all cSNPs identified here, using the PolyPhen Grid Gateway and Perl scripts

supplied by I. Adzhubey. The server reads files with SNP locations and alleles, and produces annotation files available for download. Annotation includes dbSNP rs IDs, overlapping-gene accession numbers, SNP function (for example, whether coding missense), conservation scores, HapMap minor-allele frequencies and various protein annotations (sequence, position, amino acid changes with physicochemical properties and PolyPhen classification). Indels were considered annotated by dbSNP if an entry was found with the same allele (or reverse complemented) within 1 bp of the variant position. This was to allow for ambiguities in calling the indel position.

**Calculation of genome-wide estimates.** Extrapolated estimates for the genome-wide number of cSNPs of various classes (Table 2b) were calculated based on the number of cSNP calls in that individual, the estimated sensitivity for making a variant call in that individual at any given position within the aggregate target (based on the fraction of array-based genotypes of that class that were successfully called; calculated separately for heterozygous and homozygous non-reference variants), and extrapolation to an estimated exome size of exactly 30 Mb (that is, multiplying by  $30/26.6 = 1.13$ ). A similar approach was taken to estimate the genome-wide number of uncommon cSNPs introducing non-sense codons, starting with the number observed in each individual and extrapolating based on estimated sensitivity for heterozygote detection and an estimated exome size of exactly 30 Mb.

**Freeman–Sheldon syndrome mutations.** For FSS10066, FSS22194 and FSS24895, the identified mutation was a C→T at chromosome 17:10485359, and the corresponding amino acid change was R672H. For FSS10208, the mutation was C→T at chromosome 17:10485360, and the corresponding amino acid change was R672C.